Applied Spatial Analysis and Policy (2025) 18:45
https://doi.org/10.1007/s12061-025-09649-3

Mapping Social Vulnerability to Nuclear Accidents: a Comparative Framework Using BWM and AHP Methods

Maryna Batur[1] · **Himmet Karaman**[2] · **Reha Metin Alkan**[2] · **Haluk Ozener**[3]

Received: 10 December 2024 / Accepted: 23 February 2025 / Published online: 11 March 2025
© The Author(s) 2025

Abstract

This paper examines neighborhood-scale social vulnerability to nuclear accidents in Turkiye, focusing on identifying the most at-risk areas and demographic groups across several dimensions: demographics, buildings and environment, preparedness, emergency response, and coping capacity. The study has three main objectives: (1) improving the social vulnerability model by emphasizing criteria specific to nuclear accidents, (2) developing an assessment model for identifying vulnerable communities using a worst-case nuclear accident scenario, and (3) helping emergency managers pinpoint community sub-groups most susceptible to reduced resilience. Social vulnerability was assessed using both the Best–Worst Method (BWM) and Analytic Hierarchy Process (AHP), with comparisons highlighting slight differences due to their distinct methodologies. The findings reveal significant vulnerability, with many neighborhoods lacking adequate emergency preparedness programs such as public education, access to emergency supplies, and established evacuation routes. Comparing BWM and AHP helps researchers select the most suitable method, while the developed SVI offers a valuable tool for improving nuclear disaster risk management and community resilience.

Keywords Nuclear Accident · Social Vulnerability Index · Best Worst Method · Analytic Hierarchy Process · GIS · Disaster Risk Reduction

✉ Maryna Batur
baturm20@itu.edu.tr

[1] Graduate School, Istanbul Technical University, Istanbul, Türkiye

[2] Department of Geomatics Engineering, Faculty of Civil Engineering, Istanbul Technical University, Istanbul, Türkiye

[3] Department of Geodesy, Kandilli Observatory and Earthquake Research Institute, Bogazici University, Istanbul, Türkiye

Introduction

Nuclear accidents, though rare, are catastrophic events with far-reaching consequences for public health, the environment, and social stability (Batur & Alkan, 2024). The impact of such incidents is not uniform across populations; rather, it is influenced by various social, economic, and demographic factors that determine a community's ability to prepare for, respond to, and recover from these disasters. This variability in impact is captured by the concept of social vulnerability, which reflects how different groups are more or less susceptible to harm from external stresses (Fraser & Naquin, 2022). Past nuclear accidents, such as Chernobyl in 1986 and Fukushima in 2011, have had devastating and long-lasting effects on human populations and the environment. The Chernobyl disaster, which led to widespread radioactive contamination across large parts of Europe, highlighted the vulnerabilities of rural and economically disadvantaged communities, particularly in Belarus, Ukraine, and Russia. These communities were disproportionately affected due to their limited resources, lack of access to timely information, and the economic and political challenges of the time (Batur & Alkan, 2023). The evacuation processes, health impacts, and long-term economic consequences were exacerbated by these social vulnerabilities. Similarly, the Fukushima Daiichi nuclear disaster in Japan exposed significant social vulnerabilities, especially among the elderly, rural populations, and those with limited mobility (Ohba et al., 2021). Many vulnerable individuals were unable to evacuate in a timely manner, resulting in higher exposure to radiation and prolonged displacement. The social and psychological impacts on these populations have persisted for years, further worsened by the loss of livelihoods, homes, and community ties (Fukasawa et al., 2024). Therefore, understanding social vulnerability in the context of nuclear accidents is vital for better planning and resource allocation, as well as for mitigating consequences and ensuring equitable recovery efforts.

Social vulnerability assessment has evolved significantly over the past several decades, moving from simplistic, hazard-focused approaches to comprehensive models that integrate various physical, social, economic, and demographic factors (Arda et al., 2024). Traditional models often relied on criteria-based approaches (Hadipour et al., 2020), data development analysis (Nguyen et al., 2017), or principal component analysis (Bucherie et al., 2022), using variables such as income, age, health, education, and access to services to quantify vulnerability. However, selecting and weighting these criteria has become crucial to accurately representing the complexity of social vulnerability. The application of Multi-Criteria Decision-Making (MCDM) techniques, including the Analytic Hierarchy Process (AHP) and the Best–Worst Method (BWM), has introduced a systematic approach to determining criteria weights, addressing the subjectivity and inconsistencies often associated with expert judgment and traditional statistical methods (Arda et al., 2024). These methods provide a structured framework for integrating expert opinions, ensuring that the derived indices reflect both empirical data and stakeholder perspectives.

The AHP, developed by Saaty (1977), is one of the most widely used MCDM techniques in vulnerability assessments. It facilitates decision-making by

structuring complex problems into a hierarchical model, breaking them down into criteria and sub-criteria. AHP has been applied in various studies to assess social vulnerability to different hazards. For instance, Jena et al. (2020) used AHP to construct a Social Vulnerability Index (SVI) for Northern Sumatra, incorporating expert knowledge to weight factors such as geotechnical, structural, and social elements. Similarly, Guo and Kapucu (2020) applied AHP in rural China to integrate socioeconomic and physical vulnerability criteria, demonstrating how local expertise can enhance the accuracy of vulnerability assessments.

The BWM, introduced by Rezaei (2015), is a relatively recent MCDM technique that has gained popularity in vulnerability assessments due to its efficiency and reduced cognitive burden on experts. BWM simplifies the weighting process by requiring decision-makers to identify the most and least important criteria, which are then compared against all other criteria. Like AHP, BWM has been employed in various SVI studies due to its streamlined approach. For example, Tascón-González et al. (2020) used BWM to construct an SVI for flood-prone areas in the northwest of the Iberian Peninsula, incorporating criteria of physical exposure and resistance. The method allowed for efficient and consistent weight determination, highlighting the importance of evacuation time in flood vulnerability.

In these studies, the selection of criteria often depends on data availability, the study context, and expert judgment. However, most existing studies on social vulnerability are designed for natural disasters such as floods, hurricanes, and earthquakes, and do not fully capture the specific vulnerabilities associated with nuclear accidents. For example, health criteria in natural disasters typically focus on general accessibility to healthcare centers for trauma or injury, which are usually short-term needs (Contreras et al., 2023). In contrast, health criteria for nuclear accidents must focus on ongoing healthcare provision and access to specialized radiation treatment facilities. While both natural disasters and nuclear accidents require consideration of buildings and environmental factors, the focus differs: natural disasters like earthquakes emphasize earthquake-resistant engineering (Sauti et al., 2020), while nuclear accidents prioritize radiation shielding and contamination resistance. Moreover, evacuation and mobility criteria in natural disasters often include access to outdoor assembly areas or hospitals based on potential road damage (Bakioğlu & Karaman, 2018; Frigerio et al., 2019). In nuclear accidents, however, evacuation plans must account for a safe radius from the radiation source and access to radiation-resistant shelters, based on accurate and timely meteorological information. Understanding meteorological conditions during a nuclear emergency is crucial for planning safer and more efficient evacuation routes, preventing secondary accidents or traffic congestion.

Additionally, there is a lack of studies that integrate spatial and environmental dimensions of risk with social vulnerability criteria to create a unified framework addressing both environmental exposure and social factors. In the context of a nuclear accident, this gap limits the ability to assess how radioactive pollution affects vulnerable populations and to develop targeted interventions that address both social and environmental risks. A potential solution is to apply spatially explicit radiation data to map the hazard footprint, which can be achieved using the Gaussian Plume Model. This model, widely used in environmental engineering and air

quality management, estimates the concentration of airborne contaminants emitted from point sources, such as industrial facilities or exhaust stacks (Batur et al., 2024). When integrated with social vulnerability assessments, the Gaussian Plume Model provides valuable insights into how environmental pollution impacts vulnerable populations.

To address these limitations, our research proposes developing a Social Vulnerability Index specifically tailored to nuclear accidents. We first aim to estimate radiation concentration at various distances from the source based on certain assumptions and input parameters. Then, we will conduct a social vulnerability assessment by selecting the necessary criteria and criteria based on the results of the Gaussian Plume Model simulation of a nuclear accident. Our work specifically focuses on the following objectives: (1) assessing and mapping the levels of social vulnerability within different communities that could be affected by nuclear accidents, identifying which populations are most at risk based on demographic and environmental factors; (2) identifying specific geographic areas with a high SVI score, indicating they may require more resources and attention in the event of a nuclear accident, to help plan targeted interventions; and (3) informing and enhancing emergency preparedness and response strategies by incorporating SVI data, including developing tailored evacuation plans, communication strategies, and resource allocation to ensure vulnerable populations are adequately supported. These objectives will be achieved by applying both BWM and AHP to systematically evaluate and prioritize the criteria that influence social vulnerability. The resulting SVI will provide a robust framework for identifying high-risk communities and informing disaster risk reduction strategies, ultimately contributing to improved nuclear disaster preparedness and response efforts.

The development of an SVI for nuclear accidents has significant implications for both research and practice. For researchers, this study contributes to the growing body of literature on vulnerability assessment by comparing BWM and AHP. By comparing these two methods, we can highlight their differences in terms of computational complexity, consistency of judgments, and suitability for different problem sizes, helping researchers choose the most appropriate method for their specific context. For practitioners, the SVI offers a practical tool for enhancing nuclear disaster risk management, enabling more targeted interventions that can reduce vulnerability and improve community resilience.

Materials and Methods

Study Area and Potential Environmental Contamination in the Event of an Accident

The Akkuyu Nuclear Power Plant (NPP) is situated along Turkey's Mediterranean coast in Mersin Province, approximately 140 km west of the city of Mersin and about 280 km east of Antalya, a well-known tourist destination (Fig. 1). Chosen as the site for Turkiye's first NPP, Akkuyu marks a significant step in the nation's energy infrastructure development (Tuncer et al., 2024).

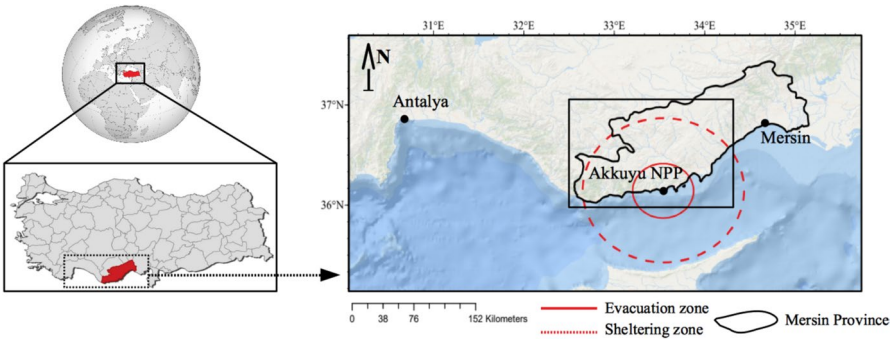

Fig. 1 Akkuyu NPP site location and neighboring areas

The relevance of the Akkuyu NPP to a social vulnerability study is multifaceted. The surrounding areas have a low population density, with small, scattered villages and towns (Batur et al., 2024). The local population is predominantly older, with many middle-aged and elderly residents who may be more vulnerable in an emergency. The economy is mainly agricultural, relying on farming, livestock rearing, and fishing, with the region being notably productive in fruits and vegetables (Orhan, 2021). However, healthcare facilities are limited, with residents primarily dependent on local clinics. In the event of a nuclear incident, providing medical care, executing evacuations, and managing public health would be major challenges.

An accident at the plant could lead to significant environmental contamination, with both immediate and long-term impacts. The severity of contamination would depend on factors like the nature of the accident, the type and amount of radioactive material released, and the weather conditions at the time (Bektaş & Lüle, 2022). The geographical spread of a radioactive material can be estimated using the Gaussian plume model, a common tool in atmospheric dispersion modeling that predicts pollutant concentration in the air following a release.

The general equation of the concentration of a pollutant at ground level and a distance x downwind is given by (1) (Aghaie et al., 2019):

$$C(x,y,0) = \frac{Q}{\sqrt{2\pi} \times u \times \sigma_y \times \sigma_z} \times exp\left(-\frac{y^2}{2\sigma_y^2}\right) \times exp\left(-\frac{H^2}{2\sigma_z^2}\right) \quad (1)$$

where Q is the release rate; u is the wind speed; H represents the effective height of the release; and σ_y and σ_z are the horizontal and vertical dispersion parameters, respectively.

The methodology used in this study closely follows our previous research (Batur et al., 2024). We used the Gaussian plume model to determine evacuation and sheltering zones based on a threshold concentration of radioactive material that poses a risk to human health. Under a worst-case accident scenario, we defined the need for immediate evacuation for residents within a 30 km radius of the NPP, while indoor sheltering is necessary for those within a 30–80 km radius. The study's scope is thus

confined to these calculated evacuation and sheltering zones (Fig. 1), with the SVI calculated at the neighborhood level.

Vulnerability Assessment Framework

Figure 2 outlines the framework for assessing social vulnerability. The research begins with defining the context and establishing the objectives, with the primary goal of identifying high-risk areas in the event of a nuclear accident. After selecting and gathering relevant criteria aligned with the study's objectives, the data were normalized to comparable scales using the min–max normalization method. Weights for each criteria were then assigned using both the BWM and the AHP. ArcGIS was employed to map the spatial distribution of social vulnerability, enabling the visualization of different neighborhoods, identifying hotspots, and pinpointing areas requiring targeted interventions. Finally, the results from both methods were compared visually and statistically.

Selection of Criteria and Data Collection

The SVI for nuclear accidents includes two key components: Physical Exposure and Resistance. Physical Exposure assesses direct exposure to hazardous conditions, while Resistance evaluates the capacity to withstand and recover from the disaster's impact. Both components are crusial for understanding and enhancing the resilience

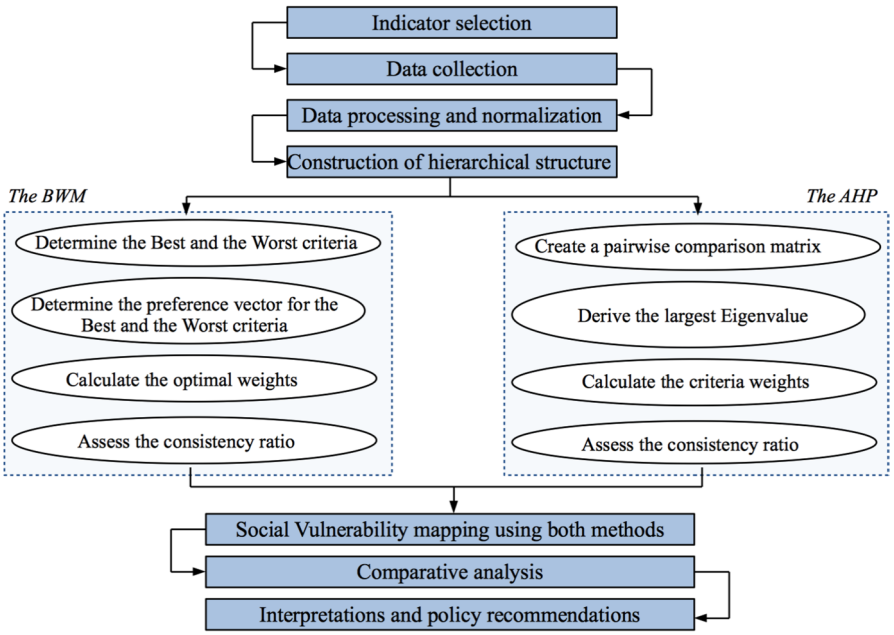

Fig. 2 Research framework for estimation and mapping of social vulnerability to nuclear accident

of individuals and communities facing such events. In our study, Physical Exposure is divided into two subcomponents: Demography and Buildings and Environmental Systems**.** Resistance is categorized into three subcomponents: Preparedness**,** Emergency Response, and Coping Capacity**.** Each subcomponent is further broken down into factors representing the overall vulnerability components. A schematic representation of these components and factors is shown in Fig. 3.

Various data sources were used to measure the SVI, including existing, objective, and subjective data. Existing data, such as population demographics from census data and environmental data like Land Use Land Cover (LULC) maps, were collected from governmental agencies. Objective data included quantifiable information, like the number of hospitals, police, and fire stations, gathered through governmental records and Geographic Information Systems (GIS). Subjective data, obtained by surveying subject-matter experts, was used to assign weights to the research criteria.

The raw data was converted into indexes and ratios, such as population density expressed as persons per square kilometer and the illiteracy rate as the proportion of the illiterate population. The data for each neighborhood was then analyzed separately using ArcGIS software.

To ensure comparability across datasets, the data was normalized using the min–max method, which scales values between 0 and 1. The first step in normalization was to identify the relationship between each factor and social vulnerability. For example, higher population density correlates with increased vulnerability, indicating a positive relationship. Conversely, an increase in medical supplies correlates with decreased vulnerability, indicating a negative relationship.

Normalization was carried out using the following Eqs. (2)-(3) (Kumar & Bhattacharjya, 2020).

For positive correlation:

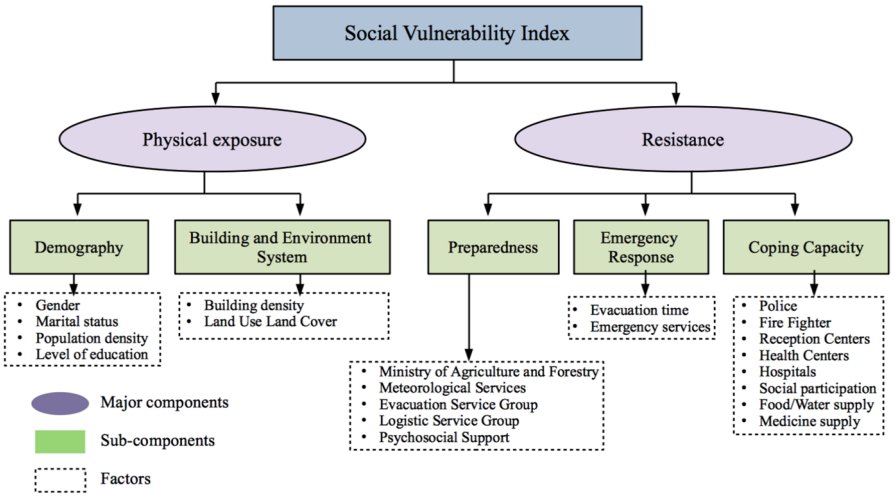

Fig. 3 The hierarchical structure of the nuclear accident vulnerability criteria used in the study

$$X_n = \frac{X - X_{min}}{X_{max} - X_{min}} \tag{2}$$

For negative correlation:

$$X_n = \frac{X_{max} - X}{X_{max} - X_{min}} \tag{3}$$

where *Xn* represents the normalized value of the factor, *X* is the actual value of the factor, *Xmin* and *Xmax* are the minimum and maximum values of the factor, respectively.

Table 1 list the subcomponents and factors selected for the study, along with their representation and relationship to vulnerability.

Gender

Including a gender criteria in the SVI for a nuclear accident study is crucial for several reasons. Gender can impact how individuals experience and respond to disasters. For example, women may face heightened risks due to societal roles, economic dependency, and specific physical vulnerabilities. Research indicates that women often have fewer resources and less access to emergency services compared to men, which can amplify their vulnerability during and after a disaster (Müller et al., 2011; Ajtai et al., 2023). Additionally, women frequently assume primary caregiving responsibilities for children, elderly family members, or individuals with disabilities. In the event of a nuclear accident, this caregiving role can exacerbate their stress and vulnerability as they manage both their own needs and those of their dependents.

Marital Status

Including marital status as an criteria in the SVI is valuable for understanding variations in household dynamics, caregiving duties, economic stability, and emotional support, all of which can affect vulnerability during a nuclear accident. Those who are married or living with a partner often share caregiving responsibilities, which can influence their response and recovery during a disaster. Conversely, single individuals may have to handle caregiving on their own, potentially increasing their vulnerability. Economically, married individuals usually benefit from dual incomes, offering greater financial stability and resources to manage the impact of a disaster. Additionally, marital status can influence living arrangements and the sharing of resources (Gayen et al., 2020).

Population Density

Incorporating population density as an criteria in the SVI helps to highlight the heightened challenges and risks present in high-density areas during a nuclear accident. In densely populated regions, traffic congestion can significantly hinder efficient evacuation and impede emergency services' ability to deliver aid. Additionally,

Table 1 Functional relationship of factors with vulnerability

Subcomponents	Factors	Representation	Correlation with vulnerability
Demography	Gender	% women = (population of women/total population) × 100	Positive
	Marital status	% single = (not married population/total population) × 100	Positive
	Population density	P.D. = total population/area	Positive
	Level of education	% illiterate = (population without education/total population) × 100	Positive
Building and Environmental System	Building density	% of buildings = (number of buildings/total area) × 100	Positive
	LULC	% agricultural areas = (agricultural areas/total area) × 100	Positive
Preparedness	Ministry of agriculture and forestry	Number per neighborhood population = ((number + (1/near distance)) / total neighborhood population	Negative
	Meteorological services		Negative
	Evacuation service group		Negative
	Logistic service group		Negative
	Psychosocial support		Negative
Emergency response	Emergency services		Negative
	Evacuation time	The time needed for individuals to reach safety areas, considering traffic congestion, was derived from network analysis conducted in a GIS environment	Positive
Coping capacity	Social participation	Number per neighborhood population = ((number + (1/near distance)) / total neighborhood population	Negative
	Food/water supply		Negative
	Medicine supply		Negative
	Police		Negative
	Firefighter		Negative
	Reception centers		Negative
	Health centers		Negative
	Hospitals		Negative

the demand for resources like medical services, emergency shelters, and supplies can quickly overwhelm available capacity, leading to potential shortages and delays in providing aid (Ajtai et al., 2023; Furlan et al., 2021).

Level of Education

Education level as an criteria offers important insights into how educational attainment impacts a person's ability to process information, access resources, and react during a nuclear accident. Individuals with higher education levels are generally better equipped to comprehend and adhere to complex emergency instructions and safety protocols, which is vital in such scenarios (Žurovec et al., 2017). In contrast, those who are illiterate may struggle to grasp the seriousness and implications of a nuclear accident, impairing their ability to make well-informed decisions in an emergency. Additionally, illiterate individuals often rely more heavily on family, friends, or community networks for information and support, which could be a significant vulnerability if these networks are disrupted or unable to provide adequate assistance during a nuclear incident (Arvin et al., 2023).

Building Density

High building density often results in crowded residential and occupational spaces, complicating evacuation efforts during a nuclear accident. Dense urban layouts can obstruct emergency responders, delaying the delivery of assistance and the execution of rescue operations. Narrow streets and congested areas further restrict the movement of emergency vehicles, impeding timely intervention (Ajtai et al., 2023; Shafapourtehrany et al., 2022).

Land Use and Land Cover

The type of land cover, such as residential, agricultural, or forested areas, plays a significant role in determining exposure levels to radiation hazards. Agricultural regions, for instance, are particularly vulnerable to widespread crop contamination, which could severely impact food security and local livelihoods (Žurovec et al., 2017). Land use is also intrinsically linked to economic activities in the area; agricultural land use suggests communities reliant on farming, which could face substantial challenges due to soil contamination. Similarly, urban land use typically involves commercial and industrial activities, where disruptions could lead to significant economic losses and increased unemployment (Fatemi et al., 2017).

Preparedness Criteria

Preparedness involves all the planning, education, and resource allocation undertaken before a nuclear accident occurs (Isia et al., 2023). In our study, preparedness includes several government services such as the Ministry of Agriculture and Forestry, Meteorological Services, Evacuation and Logistics Service Groups, and Psychosocial Support Groups. The Ministry of Agriculture is crucial in nuclear accident

preparedness due to its role in ensuring food security, protecting agricultural livelihoods, and maintaining public health through safe food production. Meteorological Services are vital for both immediate and long-term responses to nuclear accidents. Accurate weather forecasts are essential for effective emergency response planning, including identifying affected areas and planning evacuation routes and shelter locations. Evacuation and Logistics Groups are responsible for efficiently moving people to safety and ensuring that necessary support systems are in place to manage the aftermath of a nuclear accident. Their effective preparation and response are crucial for minimizing health risks and ensuring a swift recovery. Finally, Psychosocial Support Groups are essential for addressing the mental and emotional well-being of those affected by a nuclear accident, contributing to a more effective and compassionate response to the crisis (Ohba et al., 2021).

Emergency Response Criteria

Emergency response to a nuclear accident involves a coordinated approach to address both immediate and long-term effects of the incident (Ohba et al., 2021). Our study identifies key components of this response, including emergency services and evacuation time. Emergency services consist of police, firefighters, health centers, and hospitals (Isia et al., 2023). The police are crucial for maintaining safety, security, and orderly management during a nuclear accident, ensuring effective crisis handling and public protection. Firefighters play a key role in addressing immediate physical hazards, assisting with rescue operations, and supporting medical efforts, contributing to the overall effectiveness of the emergency response. Hospitals and health centers are essential in delivering immediate care, specialized treatment, and long-term support to manage both acute and chronic health issues resulting from the accident. During a nuclear accident, two key timeframes are vital for emergency response: the evacuation time and the plume arrival time. Evacuation time is the period needed to relocate individuals from dangerous areas to safe places, significantly influencing the health and safety of affected populations (Park et al., 2021). The plume arrival time refers to how long it takes for the radioactive cloud to reach nearby areas from the accident site (Smith et al., 2015). Ideally, evacuation should be completed before the plume arrives to reduce the risk of exposure to radiation. Including evacuation time in the SVI offers a more detailed understanding of how different groups are impacted by a nuclear accident. By assessing and improving evacuation times, emergency planners can better meet the needs of vulnerable populations, enhance preparedness, and mitigate the risks and effects associated with nuclear incidents (Park et al., 2021).

Evacuation Time

Evacuation time plays a crucial role in the SVI when assessing the impact of a nuclear accident. A well-planned evacuation process ensures the rapid and organized movement of people to minimize radiation exposure (Park et al., 2021). Based on the Gaussian Plume Model explained in Sect. "Study Area and Potential Environmental Contamination in the Event of an Accident" of the current study, it was determined

that residents within a 0–30 km radius of the nuclear power plant require immediate evacuation, while those living between 30–80 km should take shelter. Therefore, in this study, individuals in the 0–30 km zone are assumed to evacuate, while those in the 30–80 km zone relocate to designated shelters. To facilitate evacuation planning, we made an important assumption regarding transportation. According to regional statistical data, nearly all families in the area own private vehicles, allowing for self-evacuation (Turkish Statistical Institute, 2023). Additionally, historical nuclear accidents, such as Fukushima and Three Mile Island, have shown that almost 80% of evacuees preferred to leave using their own cars (Hasegawa et al., 2016; Wilson et al., 2023). This pattern further supports the assumption that the entire population can evacuate using private transportation. For sheltering, hospitals were chosen due to their structural advantages. Their reinforced walls, with thicknesses ranging from 0.7 to 1.0 m, provide effective radiation shielding (IAEA, 2006, 2015). These hospitals also feature underground parking spaces, which can serve as additional shelter areas if needed. Furthermore, hospitals are essential locations for conducting radiation screening before evacuees are relocated to other areas. Within the 30–80 km zone, three hospitals have been identified as potential shelters, as illustrated in Fig. 4.

Evacuation time was then calculated using the methodology outlined in Batur et al. (2025). The evacuation time estimate during a nuclear emergency is determined using the following formula (4):

$$T_{evac} = T_{mob} + T_{load} + T_{travel} + T_{clear} \tag{4}$$

where T_{mob} represents mobilization time, the period between the evacuation order and when people begin evacuating; T_{load} accounts for loading time, which includes the time taken for individuals to gather essential belongings and get into vehicles; T_{travel} refers to the travel time required to reach a safe location, depending on factors such as distance, average vehicle speed, and traffic congestions; and T_{clear} represents

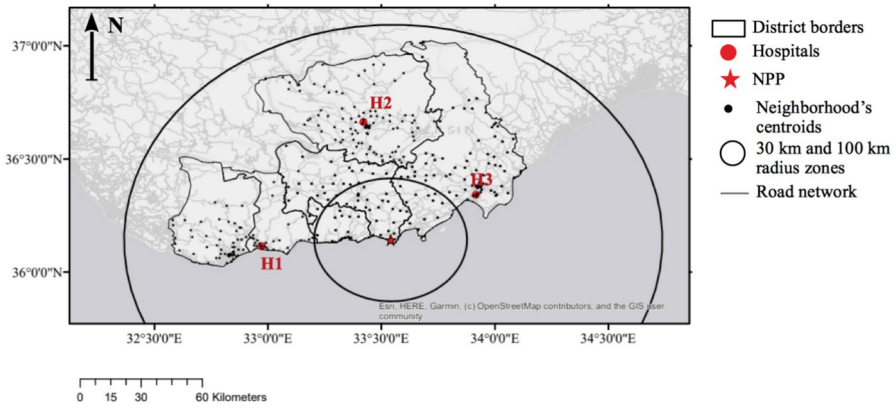

Fig. 4 Study area showing the location of Akkuyu NPP, road network, districts, neighborhoods' centroids, and the nearest hospitals to be served as an emergency destination

the road clearance time, which accounts for potential delays caused by bottlenecks, road capacity constraints, or other obstacles during evacuation.

To accurately estimate evacuation time, calculations were performed in a GIS environment using the Network Analyst tool. This tool is specifically designed for analyzing transportation networks and optimizing route planning. It evaluates the road network by considering factors such as road capacity, speed limits, and traffic congestion, enabling the identification of the most efficient evacuation routes. Network Analyst also determines the shortest paths from populated areas to designated safe locations, minimizing travel time during the evacuation process. By incorporating real-world road conditions and potential constraints, this tool provides a spatially informed assessment of evacuation efficiency, ensuring that the selected routes are practical and feasible under emergency conditions (Das et al., 2019).

The results of evacuation time calculations are shown in Fig. 5h. The disparities in evacuation time observed in the map stem from two key factors: road network limitations and GIS network analysis constraints. Within the 30-km radius of the Akkuyu NPP, the infrastructure is predominantly rural, with limited urban development and a sparse road network primarily consisting of local roads that connect small villages and towns. While some areas benefit from better road connectivity, allowing for faster evacuation, others rely on smaller, less efficient routes, leading to longer travel times. Additionally, GIS-based evacuation modeling determines the shortest evacuation path for each neighborhood. As a result, even if two adjacent neighborhoods are close, differences in road access, intersections, and alternative routes can create significant variations in evacuation time.

This analysis aligns closely with fire vulnerability literature, where evacuation efficiency is also influenced by road networks, congestion, and shelter accessibility. Studies on wildfire evacuation (e.g., Zehra & Wong, 2024) highlight how road bottlenecks and limited egress points can delay evacuation, a challenge also seen in nuclear evacuations. Similarly, fire vulnerability research has found that most evacuees prefer self-evacuation using private vehicles, reinforcing the assumption that private transportation is viable in nuclear scenarios as well (Zehra & Wong, 2024). Fire vulnerability studies also emphasize sheltering strategies, particularly the role of fire-resistant structures or designated community shelters in reducing exposure (Steer et al., 2017). This concept parallels the selection of hospitals in nuclear emergency planning due to their reinforced structures and underground facilities. Furthermore, GIS models are widely used in both fire and nuclear evacuation planning to assess spatial constraints and optimize routes (Li et al., 2019).

Coping Capacity Criteria

Coping capacity in the event of a nuclear accident encompasses effective preparedness, responsive infrastructure, community support, healthcare, recovery planning, and addressing social vulnerabilities. Strengthening these elements enables individuals and communities to handle the crisis more efficiently and recover more quickly (Isia et al., 2023; Ohba et al., 2021). In addition to emergency services such as police, firefighters, health centers, and hospitals, coping capacity also involves the efforts of volunteer organizations and communities responsible for food, water,

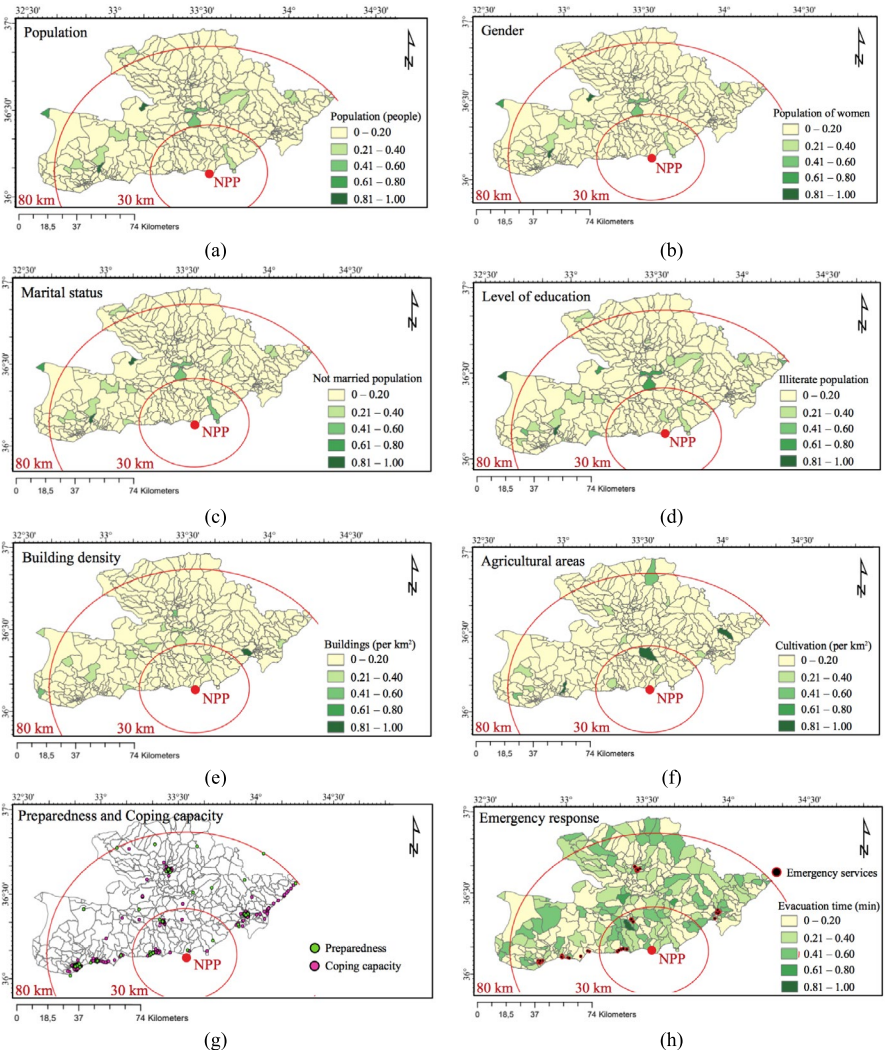

Fig. 5 Spatial representation of research criteria: **a** Population; **b** Gender; **c** Marital status;) Level of education; **e** Building density; **f** Agricultural areas; **g** Services of preparedness and coping capacity; **h** Emergency response capabilities

and medicine supply. Managing these supplies during a nuclear accident involves preventing contamination, ensuring safe availability, providing public guidance, and conducting cleanup and long-term monitoring. Volunteers play a crucial role in this process by offering hands-on support, improving coordination, and addressing both immediate and ongoing needs of those affected (Anderson et al., 2016).

During a nuclear accident, strict restrictions on food, water, and medicine are enforced to prevent radiation exposure and contamination. These restrictions are guided by national and international organizations, including the International Atomic

Energy Agency (IAEA), the World Health Organization (WHO), and the Food and Agriculture Organization (FAO) (FAO, 2011; IAEA, 2006, 2015; WHO, 2017). At the same time, urban areas are typically required to have designated emergency supply depots stocked with essential resources such as food, water, and medical supplies. These depots are established by governments, emergency management agencies, or humanitarian organizations to serve as first aid centers during disasters. Their primary purpose is to sustain affected populations during the initial response phase until larger-scale relief efforts can be mobilized (FEMA, 2019; UNDRR, 2015).

In this study, coping capacity includes factors such as access to food, water, and medical supplies. We assume that, in the event of a nuclear accident, residents will be restricted from consuming food or medicine stored in their homes or obtained from outside sources due to potential contamination. However, within the study area, several designated emergency depots are available to support the population. These depots contain non-perishable food, bottled water, emergency medical kits, and radiation protection supplies such as potassium iodide tablets (IAEA, 2006, 2015; WHO, 2017). Supplies from these depots are either distributed during evacuations or provided to individuals who may not follow official evacuation orders and choose to shelter in place. Therefore, the availability of food, water, and medical supply depots is negatively correlated with SVI. This means that the more emergency depots available, the lower the population's vulnerability, as residents will have better access to essential resources during a crisis.

Figure 5 shows the spatial representation of the research criteria selected for the study.

A region is divided into administrative units corresponding to neighborhoods. All values were classified using a normalization formula to standardize the data across the study area. The normalization process followed the methodology outlined in previous studies (e.g., Žurovec et al., 2017; Nazeer & Bork, 2019; Ajtai et al., 2023; Isia et al., 2023). Based on the normalized values, maps in Fig. 5 were categorized into five classes: 0.00–0.20, 0.21–0.40, 0.41–0.60, 0.61–0.80, and 0.81–1.00 to ensure consistency with the referenced methodologies.

Methods

Overview of the Best Worst Method

The BWM is a relatively recent MCDM approach introduced by Jafar Rezaei in 2015 (Rezaei, 2015). It is desighned to determine optimal weights for a set of criteria by comparing the most and least important criteria against all others. BWM is valued for its streamlined comparison process, which reduces cognitive effort and potential inconsistencies. Due to its efficiency, reduced comparison demand, and ability to produce consistent and reliable results, BWM has gained considerable attention.

The BWM follows these steps:

1. **Identify Criteria**: Start by listing all the criteria relevant to the decision-making problem. These criteria should cover every important aspect of the decision.

2. **Select Best and Worst Criteria**: Choose the most important criterion (Best) and the least important one (Worst) from the list.
3. **Rate the Best Criterion Against Others**: Assign values, called the Best-to-Others (BO) vector, to show how much more important the Best criterion is compared to each of the others. This is typically done using a scale from 1 to 9, where 1 means equal importance and 9 means extreme importance.
4. **Rate All Criteria Against the Worst**: Assign values, called the Others-to-Worst (OW) vector, to show how much more important each criterion is compared to the Worst.
5. **Formulate the Optimization Problem**: The goal is to find the optimal weights (w1, w2, …, wn) for the criteria. This involves minimizing the maximum difference between the weight ratios and the preference values, ensuring consistency in the decision-making process.

Mathematically, this can be expressed as (5) (Arda et al., 2024):

$$\min(w, \xi) = \xi \tag{5}$$

Subject to these constraints (6)-(8):

$$\left| \frac{w_B}{w_j} - BO_j \right| \leq \xi \forall \mathrm{j} \tag{6}$$

$$\left| \frac{w_j}{w_W} - OW_j \right| \leq \xi \forall \mathrm{j} \tag{7}$$

$$\sum_{j=1}^{n} w_j = 1, w_j \geq 0 \forall_j \tag{8}$$

here, w_B and w_W are the weights of the Best and Worst criteria, BO_j is the preference of the Best criterion over criterion j, OW_j is the preference of criterion j over the Worst, and ξ is the maximum deviation.

The solution to this optimization problem gives the optimal weights for all criteria, minimizing any inconsistencies. BWM also checks for consistency; if the consistency ratio is within an acceptable range, the weights are reliable.

Overview of the Analytic Hierarchy Process

The AHP, developed by Thomas L. Saaty in the 1970s, is a popular method for MCDM (Saaty, 1977). It helps decision-makers manage complex problems by breaking them down into a hierarchy, assessing the relative importance of various criteria, and evaluating different alternatives based on these criteria. AHP is particularly effective for decisions that involve both qualitative and quantitative factors. This method has been used in spatial decision making since 1990's (Jankowski, 1995; Malczewski, 1999). There are many different studies from disciplines from

marketing (Davies, 2001) to disaster management (Karaman & Erden, 2014) showing the vast applicability of the method.

The AHP process involves several key steps:

1. **Define the Problem and Objective**: Start by clearly articulating the decision problem and setting the main objective.
2. **Create the Hierarchy**: Organize the problem into a hierarchical structure. Place the main goal at the top, followed by criteria (and sub-criteria if necessary), and list the alternatives at the bottom.
3. **Construct Pairwise Comparison Matrices**: Compare elements in pairs to determine their relative importance. This is usually done using a scale from 1 to 9, where 1 means equal importance and 9 means one element is extremely more important than the other.
4. **Calculate Relative Weights**: Use the pairwise comparisons to determine the relative weights of each element. This involves normalizing the comparison matrices and calculating the principal eigenvector, which provides the weights for each element.
5. **Check for Consistency**: Ensure that the pairwise comparisons are consistent by calculating the Consistency Index (CI) and Consistency Ratio (CR). A CR of 0.10 or less indicates acceptable consistency; higher values suggest the need for revision.
6. **Synthesize Results**: Combine the weights of criteria and sub-criteria to rank the alternatives. Multiply the scores of the alternatives by the criteria weights and sum them to obtain a final score for each alternative.
7. **Make the Decision**: Select the alternative with the highest score as the best option.

The advantage of AHP is that it provides consensus on experts' opinions through a detailed pairwise comparison of the criteria, unlike the BWM, which relies on a simplified questionnaire.

Results

Expert Survey

Decision-making in this study was informed by the input of multiple experts, providing a comprehensive perspective. An expert in this context is defined as an individual with significant expertise in SVI analysis and disaster management, acquired through both practical fieldwork and academic training. The questionnaires were developed based on the hierarchical structure of nuclear accident vulnerability criteria.

The survey included 25 participants, primarily selected from universities. Of these participants, 77% were from the Geomatics Engineering department, which included GIS and disaster management experts, 14% were from Environmental and

Earth Sciences, and 9% were from the Nuclear Engineering department. This diverse panel allowed for a range of viewpoints, avoiding reliance on a single perspective for deriving solutions. The results were then assessed using the consistency ratio.

Figure 6 presents the box plots of the final weights for each criterion, providing a visual comparison of how these weights are distributed using two different methods. The descriptions of the criteria are detailed in Table 2.

In the BWM, the weights vary significantly across different criteria. Some criteria, such as D3 and R1, have higher weights and a broader dispersion, indicating greater variability in their perceived importance. On the other hand, criteria like P1 and P5 have lower and more narrowly distributed weights, suggesting they are considered less significant and evaluated more consistently.

For the AHP, a similar variability in weights is observed, although the distributions differ slightly from those in BWM. While criteria like D3 and R1 still have higher weights, the overall spread may differ somewhat from the BWM results.

SVI Obtained with BWM

The SVI map was created by ranking vulnerable areas based on the factors and components outlined in Sect. "Selection of Criteria and Data Collection". Social vulnerability is classified into five categories: very low, low, moderate, high, and very high. These five levels of vulnerability are also represented on a color scale in Fig. 7, enhancing the visual distinction between the different degrees of risk.

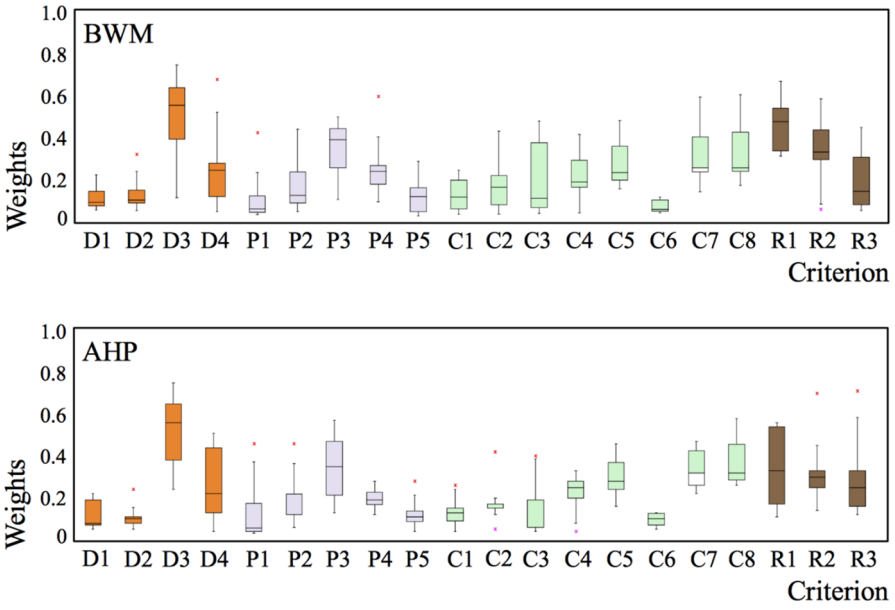

Fig. 6 Dispersion of weights for each criterion

Table 2 Description of criteria which shown in Fig. 6

Name	Description	Name	Description	Name	Description	Name	Description
D1	Gender	P2	Meteorological services	C2	Food/water supply	C7	Health centers
D2	Marital status	P3	Evacuation service group	C3	Medicine supply	C8	Hospitals
D3	Population density	P4	Logistic service group	C4	Police	R1	Preparedness
D4	Level of education	P5	Psychosocial support	C5	Firefighter	R2	Emergency response
P1	Ministry of agriculture and forestry	C1	Social participation	C6	Reception centers	R3	Coping capacity

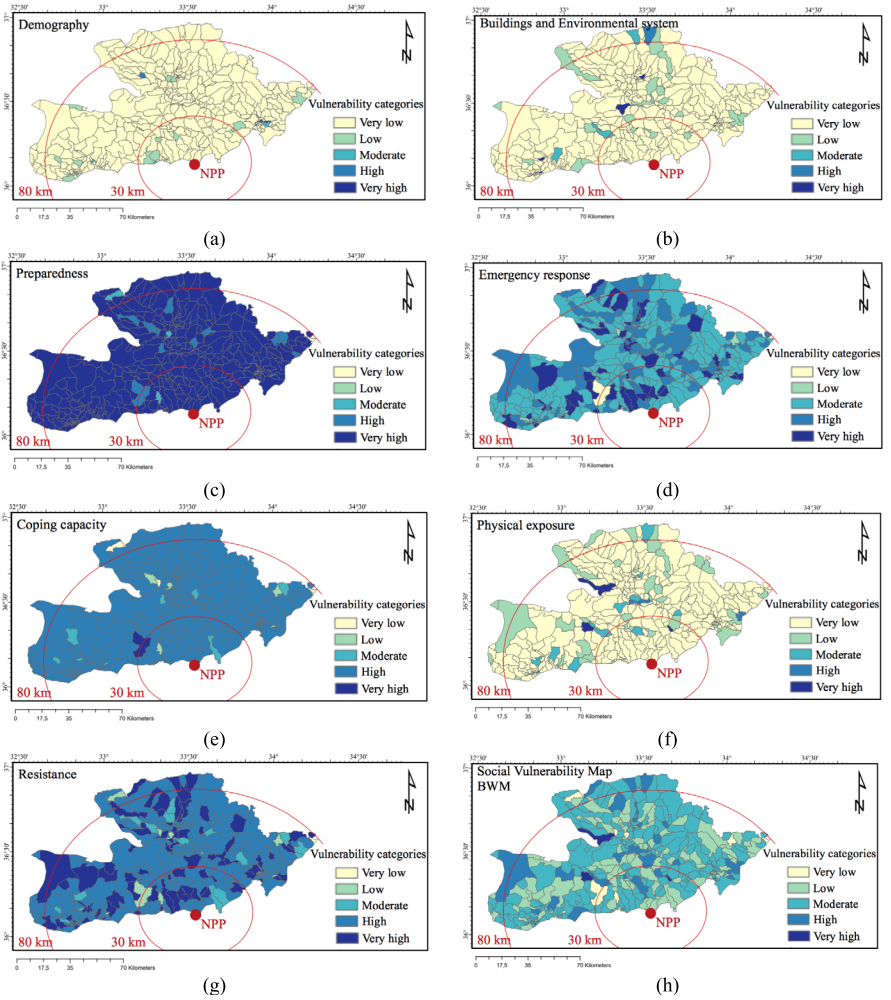

Fig. 7 Social vulnerability coefficient maps obtained with BWM: **a** Demography map; **b** Building and environmental system map; **c** Preparedness map; **d** Emergency response map; **e** Coping capacity map; **f** Physical exposure map; **g** Resistance map; **h** SVI map

Social vulnerability levels in the context of a nuclear accident were assessed using various criteria, as shown in Fig. 7. The demographic vulnerability map (Fig. 7a) indicates that the entire study region predominantly exhibits a low SVI. This is largely due to the uniform distribution of women across the area, a lower percentage of single individuals compared to married ones, a low illiteracy rate, and a generally low population density. These factors contribute to the demographic resilience of the area, thereby reducing the potential impact on the population in the event of a nuclear incident.

Similar results are observed in the building and environmental vulnerability map (Fig. 7b), which evaluates the physical characteristics of infrastructure, land use,

and environmental conditions. The findings suggest that most of the region displays low vulnerability levels, likely due to low-density housing and minimal exposure to environmental hazards such as proximity to industrial zones or floodplains. This implies that the physical environment does not significantly increase vulnerability in the context of a nuclear accident.

The physical exposure map (Fig. 7f), which combines demographic and building/environmental data, also reveals predominantly low or very low SVI levels across the study area. Only a small proportion of regions show moderate to high vulnerability indexes, indicating that a minimal percentage of the area would be directly affected by demographic or environmental factors during a nuclear event.

However, a different trend emerges when examining the preparedness, emergency response, and coping capacity maps (Fig. 7c, d, and e). These maps show the highest SVI values across the study area, highlighting critical weaknesses in the region's ability to respond to and manage the consequences of a nuclear accident. The emergency response map, in particular, reveals high vulnerability due to maximum exposure values associated with the evacuation time criteria. This analysis indicates that in many areas, the time required for residents to evacuate the hazardous zone exceeds the time needed for a radioactive plume to reach the region, creating a severe risk to public safety. Moreover, the resistance map (Fig. 7g), which reflects the capacity of the region to withstand or recover from adverse events, does not sufficiently mitigate these vulnerabilities. The high SVI values for preparedness and coping capacity cannot be adequately countered due to the limited effectiveness of these criteria, suggesting that current emergency management strategies are inadequate in reducing high exposure risks.

The final SVI map (Fig. 7h) synthesizes these findings, showing that a significant number of neighborhoods within the study area are likely to experience moderate to high levels of social vulnerability in the event of a nuclear accident. This elevated vulnerability is primarily driven by deficiencies in preparedness, emergency response, and coping capacity rather than by demographic or environmental factors alone. These results underscore the urgent need for targeted interventions, such as improving emergency response infrastructure, enhancing public preparedness programs, and developing comprehensive evacuation strategies to protect vulnerable populations from potential nuclear hazards.

SVI Obtained with AHP

The SVI map, generated using the AHP, is presented in Fig. 8. This map assesses the vulnerability of various regions by integrating factors from demographic and building/environmental data, preparedness, emergency response, and coping capacity. The physical exposure map (Fig. 8f), derived by combining demographic and building/environment maps (Fig. 8a and b), shows minimal deviation from the results obtained through the BWM. Neighborhoods with very low or low vulnerability are primarily found in areas with a discontinuous urban fabric. These areas generally exhibit reduced vulnerability associated with LULC due to

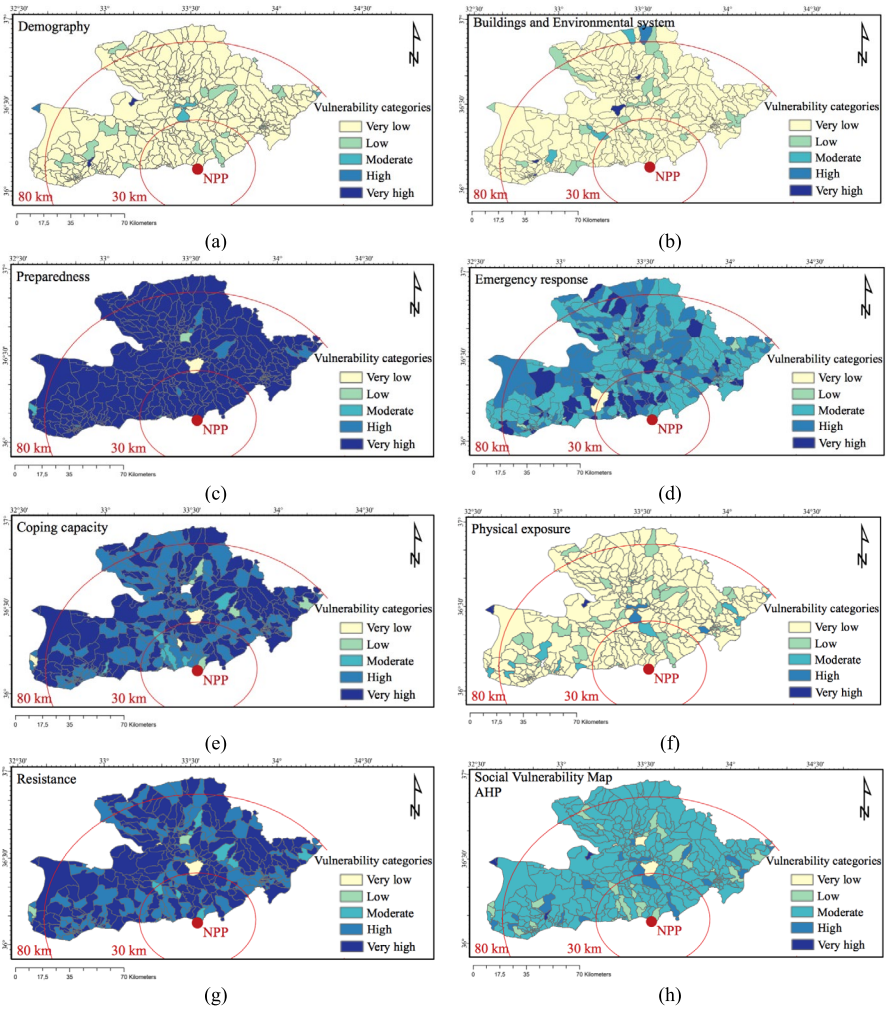

Fig. 8 Social vulnerability coefficient maps obtained with AHP: **a** Demography map; **b** Building and environmental system map; **c** Preparedness map; **d** Emergency response map; **e** Coping capacity map; **f** Physical exposure map; **g** Resistance map; **h** SVI map

a lower percentage of residing populations, fewer buildings, and lower housing density. Consequently, these zones contribute less to the overall social vulnerability in the region.

The resistance map (Fig. 8g), which evaluates the ability of an area to withstand or recover from adverse events, indicates higher vulnerability levels compared to those obtained using BWM. This is particularly evident in areas within a 30-km radius of the NPP, where nearly all zones are classified as having very high vulnerability levels. This classification suggests that these areas are at significant risk, particularly in the context of a nuclear accident. Approximately 90%

of the zones within this radius are categorized as high or very high in vulnerability, highlighting the urgent need for targeted risk mitigation strategies in these regions.

The final SVI map (Fig. 8h) reveals that most regions fall into the moderate vulnerability category, with several neighborhoods displaying low vulnerability scores. Interestingly, the neighborhoods with lower vulnerability are often located in close proximity to the NPP. This somewhat counterintuitive finding can be attributed to higher levels of regional development, which includes economic prosperity, denser road networks, and the presence of governmental institutions. These factors significantly enhance the quality of public infrastructure, thereby reducing vulnerability levels in these areas. Enhanced economic development in these regions ensures better access to community services, improved disaster response capabilities, and greater resilience, ultimately making these areas less vulnerable despite their geographic proximity to the NPP.

The presence of well-developed public infrastructure, such as hospitals, emergency services, and robust transportation networks, plays a crucial role in reducing social vulnerability. Additionally, better road density facilitates quicker evacuation and access to emergency services, while governmental institutions contribute to more effective disaster management policies and practices. As a result, regions with higher economic development are better equipped to respond to and recover from potential nuclear accidents, emphasizing the importance of continued investment in infrastructure and regional development to mitigate social vulnerability.

These findings underscore the complex interplay between physical, social, and economic factors in shaping social vulnerability. While demographic and environmental characteristics play a significant role, the level of regional development and the availability of critical infrastructure are key determinants in reducing vulnerability, particularly in high-risk areas near nuclear facilities. This highlights the need for comprehensive planning and investment in regional development as a critical component of nuclear accident preparedness and response strategies.

Statistical Comparison of BWM and AHP

Wilcoxon Signed-Rank Test

To assess whether there is a statistically significant difference between the BWM and the AHP, the Wilcoxon Signed-Rank test was applied. This non-parametric test is ideal for comparing two related samples, particularly when the data is ordinal or not normally distributed, unlike the paired t-test, which assume a normal distribution of differences between pairs (Taheri & Hesamian, 2013). The test evaluates the differences between the weights assigned by BWM and AHP, respectively, for the same criterion, using the Eq. (9):

$$d_i = x_i - y_i \tag{9}$$

where x_i is weight assigned by BWM and y_i is weight assigned by AHP.

After removing zero differences, the absolute values of d_i are ranked, with ranks assigned signs based on the direction of d_i. The test statistic W is the smaller of the sums of positive (W^+) and negative (W^-) ranks. For small samples ($N<25$), W is compared to critical values; for larger samples, it is approximated using a normal distribution as shown in Eq. (10):

$$Z = \frac{W - \frac{n/(n/+1)}{4}}{\frac{n/(n/+1)(2n/+1)}{24}} \tag{10}$$

where W is the test statistic, and $n/$ is the effective sample size (after removing zero differences).

The p-value derived from Z determines whether the null hypothesis (no difference) is rejected at a chosen significance level (e.g., $\alpha=0.05$). In this study, the test was applied to compare weight distributions across criteria, providing insights into the consistency and potential biases of BWM and AHP in social vulnerability assessment. A significant difference suggests methodological divergence, while no difference indicates comparable effectiveness. The results of this analysis are presented in Table 3.

The difference in medians (0.42 for BWM and 0.46 for AHP) indicates that the values obtained using the AHP method are generally higher than those obtained using BWM. The Z-value of 15.7 is notably high, signaling a significant difference between the ranks of the two datasets. This suggests that the observed difference between the two methods is not due to random chance. Moreover, the p-value is less than 0.001, indicating there is less than a 0.1% probability that this difference occurred by chance. The large effect size further confirms that the difference between BWM and AHP is not only statistically significant but also practically meaningful. Thus, the shift from BWM to AHP has a substantial impact on the measured outcomes.

The observed differences in assessing social vulnerability using BWM and AHP arise from their distinct methodological approaches. BWM focuses on directly comparing the "best" and "worst" criteria, resulting in a more stable but potentially less detailed assessment, as it tends to be less sensitive to small changes in criteria rankings. In contrast, AHP requires pairwise comparisons between all criteria, leading to a more detailed and comprehensive assessment of the relative importance of each factor. AHP' sensitivity to changes in individual pairwise comparisons can result in different outcomes, particularly when criteria are closely ranked or when respondents' judgments vary slightly.

Table 3 The results of wilcoxon signed-rank test

Method	N	Median	Min	Max	Test statistics Z	*p*-value	Effect size r
BWM	347	0.42	Low	High	15.70	<0.001	0.85
AHP	347	0.46	Very low	Very high			

Literature comparing BWM and AHP methods often highlights the superior reliability of AHP, owing to its detailed pairwise comparison process and built-in consistency validation. For instance, Ortega et al. (2021) reported that AHP produced more consistent and reproducible results in a study on decision-making methods for facility location problems. Similarly, Singh and Pant (2021) emphasized that AHP's capability to accurately model and validate complex decision structures made it the preferred approach in multi-criteria assessments.

Sensitivity Analysis

In MCDM processes, sensitivity analysis plays a crucial role in assessing the robustness and reliability of results by evaluating how variations in input parameters affect the final outcomes (Asare et al., 2024). Given that methods such as the BWM and AHP rely on subjective expert judgments and weighting schemes, sensitivity analysis helps determine whether small changes in criteria weights significantly alter the rankings or decisions. If the results remain stable despite variations in input values, the model is considered robust; otherwise, adjustments may be needed to improve its reliability. Sensitivity analysis typically involves systematically modifying the weights assigned to different criteria while observing the impact on the final ranking of alternatives or solutions. One of the most effective ways to visualize these changes is through a tornado chart, which graphically represents how variations in each criterion's weight influence the overall ranking. The tornado chart displays horizontal bars corresponding to different criteria, with the length of each bar indicating the extent to which changes in that criterion affect the final result. Criteria with longer bars exert a greater influence on the decision, highlighting key factors that drive the outcome. This visualization is particularly useful in identifying which parameters require the most careful consideration during decision-making.

Mathematically, sensitivity analysis can be performed by introducing a perturbation factor Δw_j to the original weight w_j of each criterion and recalculating the final scores. A general formula can be expressed as (11):

$$w_j^{/} = w_j + \Delta w_j \tag{11}$$

where $w_j^{/}$ is the perturbed weight of criterion j, w_j is the original weight of criterion j, and Δw_j is the perturbation factor applied to w_j.

After adjusting the weights, the final score $S_i^{/}$ for each alternative i can be recalculated using a weighted sum model as shown in Eq. (12):

$$S_i^{/} = \sum_{j=1}^{n} w_j^{/} x_{ij} = \sum_{j=1}^{n} \left(w_j + \Delta w_j\right) x_{ij} \tag{12}$$

where $S_i^{/}$ is the updated score for alternative i, x_{ij} is the performance value of alternative i under criterion j, and n is the total number of criteria.

In our study, to check the robustness of decision-making methods, we performed sensitivity analysis by altering the criteria weights and observing how the ranking of alternatives changes. Figure 9 displays a tornado graph which compares the

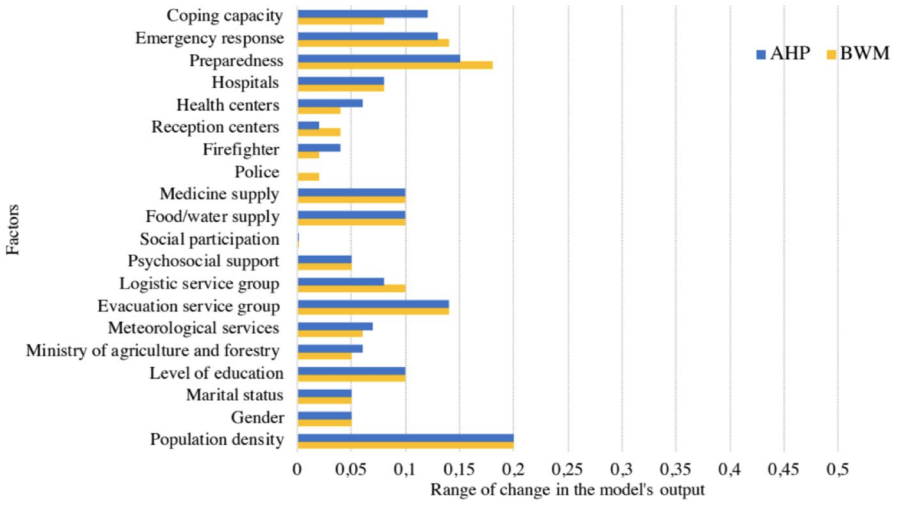

Fig. 9 The Tornado chart

sensitivity of various factors influencing a model's output using BWM and AHP. From the results, "coping capacity" and "emergency response" show the highest sensitivity for both BWM and AHP. These factors have the most significant impact on the model's outcome, indicating they are srusial in determining system performance under different conditions. "Evacuation service group" also plays a vital role, showing relatively high sensitivity. For the most factors, the BWM and AHP methods display similar ranges of sensitivity. However, there are very slights differences in some cases: "preparedness" shows a higher sensitivity in BWM compared to AHP, which suggests that BWM might consider this factor more influential than AHP; "social participation" and "police centers" show minimal impact across both methods, implying that these factors have little influence on the overall model.

Hot and Cold Spot Analysis

Understanding the spatial distribution of social vulnerability is crucial for effective disaster risk management and emergency planning. While composite indices provide an overall measure of vulnerability, they do not capture how vulnerability is spatially clustered or dispersed within a study area. To address this, a hot and cold spot analysis can be conducted using the Getis-Ord G_i^* statistic, which identifies statistically significant spatial clusters of high (hot spots) and low (cold spots) values in the composite social vulnerability index. This method helps reveal geographic patterns, allowing decision-makers to prioritize areas that require immediate attention in disaster preparedness and resource allocation (Connors & Zhang, 2023).

The Getis-Ord G_i^* statistic measures local spatial autocorrelation, determining whether high or low values of a variable, such as social vulnerability, are clustered in space. Unlike global spatial autocorrelation measures such as Moran's I, which evaluate overall spatial dependence, the Getis-Ord G_i^* statistic focuses on local

variations, identifying specific regions where social vulnerability is significantly high or low. Mathematically, the Getis-Ord G_i^* statistic for a given location i is computed using Eq. (13):

$$G_i^* = \frac{\sum_{j=1}^{n} w_{ij} x_j}{\sum_{j=1}^{n} x_j} \tag{13}$$

where x_j represents the social vulnerability index value at location j, w_{ij} is the spatial weight between locations i and j, and n is the total number of locations in the study area.

To determine the statistical significance of hot and cold spots, the Getis-Ord G_i^* statistic is standardized using a Z-score, calculated as (14):

$$Z\left(G_i^*\right) = \frac{G_i^* - E\left(G_i^*\right)}{StdDev\left(G_i^*\right)} \tag{14}$$

where the expected value $E\left(G_i^*\right)$ and standard deviation $StdDev\left(G_i^*\right)$ are defined as (15)-(16):

$$E\left(G_i^*\right) = \frac{\sum_{j=1}^{n} w_{ij}}{n} \tag{15}$$

$$StdDev\left(G_i^*\right) = \sqrt{\frac{\sum_{j=1}^{n} w_{ij}^2}{n} - \left(\frac{\sum_{j=1}^{n} w_{ij}}{n}\right)^2} \tag{16}$$

A positive Z-score indicates clustering of high social vulnerability values (hot spots), while a negative Z-score suggests clustering of low values (cold spots). The significance of the clustering is assessed using p-values, where a low p-value (e.g., $p < 0.05$) confirms that the identified hot or cold spot is statistically significant and unlikely to have occurred by chance.

In this study, hot and cold spot analysis was conducted on the composite index for social vulnerability to evaluate the degree of spatial correlation across the study area. The Getis-Ord G_i^* statistic was employed to reveal the spatial patterns in social

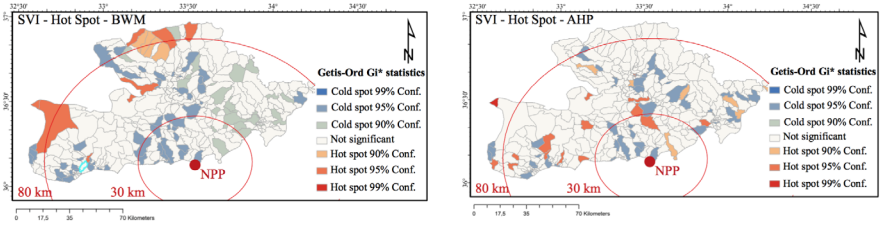

Fig. 10 Hot and cold spots of social vulnerability: **a** BWM; **b** AHP

vulnerability. Statistically significant z-scores were used to identify and visualize hot and cold spots at the 99%, 95%, and 90% confidence levels. Figure 10a and b present the results of the Getis-Ord Gi* analysis, corresponding to the BWM and AHP methods, respectively.

The red regions indicate statistically significant hot spots, representing areas with a high concentration of SVI at the 90% and 95% confidence levels. Conversely, the blue regions denote statistically significant cold spots, where the SVI is less concentrated, also identified at the 90% and 95% confidence levels. The gray areas do not display statistically significant clustering, suggesting a lack of strong spatial patterns in social vulnerability distribution in these regions.

Overall, this analysis highlights spatial patterns where specific areas, such as hot spots, exhibit a high concentration of social vulnerability. These findings are critical for informing regional planning, guiding resource allocation, and enhancing risk management strategies. They suggest the need for targeted interventions, focused policy efforts, and further research in identified hot spot regions.

Discussions

The importance of developing an SVI in the context of a nuclear accident is especially significant for countries like Turkiye, where nuclear power is being introduced for the first time. By quantifying the susceptibility of different populations to the adverse effects of a nuclear event, the SVI becomes an essential tool for guiding and improving every phase of the disaster management cycle: mitigation, preparedness, response, and recovery (Oktari et al., 2020).

In the mitigation phase, the SVI is crucial for identifying regions and populations most at risk in the event of a nuclear accident. It highlights areas with high social vulnerability, such as communities with low education levels, limited healthcare access, or poor infrastructure. This information enables policymakers to prioritize risk reduction efforts, such as targeted public education campaigns on nuclear safety. By proactively addressing these vulnerabilities, the potential impact of a nuclear disaster can be significantly reduced, thus lowering the overall risk to society (Arifah et al., 2019).

During the preparedness phase, the SVI informs the development of emergency response plans and public safety strategies. By identifying the most vulnerable populations, authorities can tailor their communication, training, and resource allocation efforts. For example, evacuation plans can be designed with special considerations for disadvantaged groups who may face greater challenges during a nuclear incident. Moreover, the SVI guides the distribution of emergency resources, ensuring that shelters, medical facilities, and supplies are accessible to those who need them most, thereby enhancing overall preparedness (Oloruntoba et al., 2018).

In the response phase, the SVI becomes a vital asset in the immediate aftermath of a nuclear accident. Emergency responders can use the index to prioritize aid and services for the most vulnerable populations, ensuring that those at the highest risk receive assistance first. This might involve deploying medical teams to areas with high concentrations of vulnerable individuals or directing evacuation efforts to

regions where social vulnerability is greatest, thereby ensuring an efficient and equitable response (Arifah et al., 2019).

Finally, in the recovery phase, the SVI guides long-term rebuilding and rehabilitation efforts. It helps identify which communities will need the most support to return to normalcy after a nuclear accident. Recovery plans can then be tailored to address the specific needs of vulnerable populations, such as providing mental health services, restoring livelihoods, or rebuilding critical infrastructure. By focusing on these areas, the recovery process becomes more effective and inclusive (Oloruntoba et al., 2018).

In our study, we used both the BWM and the AHP to assess social vulnerability to nuclear accidents at the neighborhood level. The analysis revealed different dimensions of vulnerability, particularly in terms of physical exposure and resilience capacities. The results indicated low vulnerability indexes related to physical exposure, primarily due to the geographical and demographic characteristics of these neighborhoods. They are mostly located in areas with low population density and sparse building distribution, which naturally leads to lower physical exposure in the event of a nuclear accident. Moreover, the spatial distribution of these neighborhoods, often situated away from high-risk zones like industrial areas or nuclear facilities, further mitigates physical exposure. However, when evaluating the neighborhoods' resistance to a nuclear accident, the study revealed high levels of vulnerability. This is mainly due to deficiencies in preparedness, response, and coping capacities. Many neighborhoods lack adequate emergency preparedness programs, such as public education on nuclear risks, access to emergency supplies, and well-established evacuation routes. The response capacity – local emergency services' ability to act swiftly during a nuclear incident – is also compromised due to limited resources and infrastructure. Furthermore, the ability of a community to recover from a disaster, or coping capacity, is often hindered by socioeconomic factors, such as limited healthcare access and weaker social support networks. These gaps exacerbate overall vulnerability, despite the relatively low physical exposure.

These findings highlight the complex nature of social vulnerability to nuclear accidents, where low physical exposure does not necessarily equate to lower overall risk. The critical gaps in preparedness, response, and coping capacities point to a need for targeted interventions to enhance resilience at the neighborhood level. Such interventions could include community-based education programs, investment in emergency infrastructure, and the development of comprehensive disaster management plans tailored to the unique needs of each neighborhood. Addressing these factors will help reduce overall vulnerability and improve the safety and resilience of these communities in the face of potential nuclear accidents.

Our findings align with previous studies emphasizing the critical role of socioeconomic, physical, and resistance factors in determining vulnerability. For instance, demographics such as high population density, high percentage of women, and low educational levels have been identified as significant contributors to vulnerability in various contexts (Ajtai et al., 2023; Furlan et al., 2021; Kumar & Bhattacharjya, 2020). Shafapourtehrany et al. (2022) and Ajtai et al. (2023) highlighted that areas with dense building concentrations face heightened vulnerability; a trend echoed by Žurovec et al. (2017), who linked social vulnerability to

LULC patterns in risk-prone zones. Additionally, coping capacity, response, and preparedness significantly influence SVI, as they determine the ability of communities to mitigate, adapt, and recover from hazards (Isia et al., 2023).

Understanding the methodological differences between AHP and BWM is essential for interpreting the results of the SVI. AHP often shows higher vulnerability levels due to its detailed pairwise comparisons, which can intensify subjective biases and sensitivity to criteria importance (Abdrabo et al., 2023; Xie & Meng, 2023). In contrast, BWM, with its streamlined comparison process, typically produces more balanced and moderate assessments (Debnath et al., 2023). Recognizing these nuances is crucial for making informed decisions based on the SVI in the context of nuclear accidents.

Several limitations should be considered when interpreting the results of this study. Expert surveys, which underpin both the BWM and the AHP, inherently carry potential biases, including subjectivity and variability in expert judgment. These biases can arise from differences in individual expertise, personal experiences, or cognitive biases, leading to inconsistencies in weighting criteria. Moreover, group dynamics and consensus-driven approaches may sometimes dilute individual expert opinions, affecting the robustness of the final rankings and decisions (Kazibudzki, 2021; Starczewski, 2023). Additionally, the validation of SVI predictions remains a challenge, as there is limited empirical evidence directly linking SVI scores to real-world disaster outcomes, making it difficult to assess the index's accuracy in predicting adverse impacts (Bakkensen et al., 2017). While the index provides a structured framework for assessing vulnerability, future research should aim to compare SVI predictions with real-world disaster outcomes to enhance its reliability (Rufat et al., 2019). Furthermore, the use of neighborhood-level data, while beneficial for regional analysis, may lack the granularity needed to capture vulnerability variations within smaller population groups. This limitation can obscure critical intra-community disparities, such as differences in socioeconomic conditions, resource accessibility, and building infrastructure, all of which influence vulnerability. More detailed demographic, health, and mobility data could refine the model's accuracy and improve its applicability in targeted disaster response planning. However, even when finer-scale data is available, it may introduce uncertainty due to smaller sample sizes, reporting inconsistencies, or privacy constraints (He & Guan, 2024; Tate, 2012). Future research could explore spatial interpolation, machine learning, or Bayesian approaches to mitigate these uncertainties and enhance data reliability. Additionally, social vulnerability is not static; it evolves over time due to demographic shifts, policy changes, and infrastructure development (Fekete, 2019). Incorporating time-series data and dynamic modeling approaches could improve predictive accuracy and allow for adaptive disaster response strategies. To further strengthen the robustness of SVI assessments in nuclear accident scenarios, empirical validation should be prioritized by comparing index predictions with real-world disaster impact data from past nuclear accidents, such as Fukushima or Chernobyl. Conducting case studies or retrospective analyses could provide valuable insights into the effectiveness of SVI in predicting adverse outcomes and guiding preparedness efforts.

Conclusions

This study has successfully developed and applied an SVI for nuclear accidents in Turkiye, utilizing a comparative framework of the BWM and the AHP. By evaluating neighborhoods' vulnerability across various dimensions – including demographics, buildings and environment, preparedness, emergency response, and coping capacity – this research provides critical insights into the factors that heighten social vulnerability to nuclear accidents. The comparison between BWM and AHP revealed slight variations in outcomes, attributed to their differing methodological approaches. However, both methods proved effective in identifying the most vulnerable areas and demographic groups, offering researchers and practitioners valuable tools for refining risk assessments.

From a practical standpoint, the findings emphasize the urgent need for improving nuclear emergency preparedness, particularly in neighborhoods with high vulnerability. This includes expanding public education on nuclear risks, enhancing access to emergency supplies, and developing well-defined evacuation routes. Furthermore, the SVI developed here can support emergency managers in making informed decisions to target interventions, reduce vulnerability, and bolster community resilience in the face of potential nuclear accidents.

Ultimately, this study not only contributes to the body of knowledge on social vulnerability assessment but also provides a practical, adaptable framework that can be applied to other contexts where nuclear disaster risk management is a priority. Future research should explore the integration of additional vulnerability criteria and the application of the SVI in other geographical areas to further refine and validate the model.

Acknowledgements This research was conducted as part of the first author's Ph.D. study at Istanbul Technical University. The first author is sincerely thankful to the individuals who contributed to the development and distribution of the questionnaire, without whom this research would not have been possible.

Author Contributions Maryna Batur: an idea for the research, conceptualization, data acquisition and GIS analysis, writing the first draft. Himmet Karaman: study curation, conceptualization, questionnaire design, data acquisition, validation of results, review and editing. Reha Metin Alkan: study curation, distribution of questionnaire, validation of results, revision and editing. Haluk Ozener: validation and improving of final results. All authors have read and agreed to the published version of the manuscript.

Funding Open access funding provided by the Scientific and Technological Research Council of Türkiye (TÜBİTAK). The authors declare that no funds, grants, or other support were received during the preparation of this manuscript.

Data Availability The data utilized in this study were obtained from publicy available open-source platforms. The population data used in this study were obtained from the Turkish Statistics Institute. Road network data were sourced from OpenStreetMap, while data on buildings and services were derived from Google Earth. Land Use Land Cover data were obtained from the Land Service of Copernicus, part of the Earth Observation Programme of the European Commision.

Declarations

Conflict of Interest The authors declare no conflict of interest.

Open Access This article is licensed under a Creative Commons Attribution 4.0 International License, which permits use, sharing, adaptation, distribution and reproduction in any medium or format, as long as you give appropriate credit to the original author(s) and the source, provide a link to the Creative Commons licence, and indicate if changes were made. The images or other third party material in this article are included in the article's Creative Commons licence, unless indicated otherwise in a credit line to the material. If material is not included in the article's Creative Commons licence and your intended use is not permitted by statutory regulation or exceeds the permitted use, you will need to obtain permission directly from the copyright holder. To view a copy of this licence, visit http://creativecommons.org/licenses/by/4.0/.

References

Abdrabo, K. I., Kantoush, S. A., Esmaiel, A., Saber, M., Sumi, T., Almamari, M., & Ghoniem, S. (2023). An integrated criteria-based approach for constructing an urban flood vulnerability index as an urban decision-making tool using the PCA and AHP techniques: A case study of Alexandria, Egypt. *Urban Climate, 48*, 101426. https://doi.org/10.1016/j.uclim.2023.101426

Aghaie, M., Minuchehr, A., & Alahyarizadeh, G. (2019). Evaluation of atmospheric dispersion of radioactive materials in a severe accident of the BNPP based on Gaussian model. *Progress in Nuclear Energy, 113*, 114–127. https://doi.org/10.1016/j.pnucene.2019.01.019

Ajtai, I., Ștefănie, H., Maloș, C., Botezan, C., Radovici, A., Bizău-Cârstea, M., & Baciu, C. (2023). Mapping social vulnerability to floods. A comprehensive framework using a vulnerability index approach and PCA analysis. *Ecological Indicators, 154*, 110838. https://doi.org/10.1016/j.ecolind.2023.110838

Anderson, D., Prioleau, P., Taku, K., Naruse, Y., Sekine, H., Maeda, M., & Yanagisawa, R. (2016). Post-traumatic stress and growth among medical student volunteers after the March 2011 disaster in Fukushima, Japan: Implications for student involvement with future disasters. *Psychiatric Quarterly, 87*(2), 241–251. https://doi.org/10.1007/s11126-015-9381-3

Arda, T., Bayrak, O. C., Uzar, M. (2024). Analyzing coastal vulnerability using analytic hierarchy process and best-worst method: A case study of the Marmara Gulf Region. *Arabian Journal for Science and Engineering*, 1–19. https://doi.org/10.1007/s13369-024-09128-w

Arifah, A. R., Tariq, M., & Juni, M. H. (2019). Decision making in disaster management cycle of natural disasters: A review. *International Journal of Public Health and Clinical Sciences, 6*(3), 1–18. https://doi.org/10.32827/ijphcs.6.3.1

Arvin, M., Beiki, P., & Shahraki, S. Z. (2023). A neighborhood-level analysis of association between social vulnerability and COVID-19 in Ahvaz, Iran. *International Journal of Disaster Risk Reduction, 85*, 103504. https://doi.org/10.1016/j.ijdrr.2022.103504

Asare, P., Atun, F., & Pfeffer, K. (2024). Spatial Multi-Criteria Analysis for discovering nature-based solutions location for urban flood mitigation in Accra. *Applied Spatial Analysis and Policy, 17*(1), 207–239. https://doi.org/10.1007/s12061-023-09541-y

Bakioğlu, G., & Karaman, H. (2018). Accessibility of medical services following an earthquake: A case study of traffic and economic aspects affecting the Istanbul roadway. *International Journal of Disaster Risk Reduction, 31*, 403–418. https://doi.org/10.1016/j.ijdrr.2018.05.018

Bakkensen, L. A., Fox-Lent, C., Read, L. K., & Linkov, I. (2017). Validating resilience and vulnerability indices in the context of natural disasters. *Risk Analysis, 37*(5), 982–1004. https://doi.org/10.1111/risa.12677

Batur, M., Alkan, R. M. (2023). What can we learn from past nuclear accidents? A comparative assessment of emergency response to accidents at the Three Mile Island, Chernobyl, and Fukushima Nuclear Power Plants. *Advanced Land Management*, *3*(2), 76–89. https://publish.mersin.edu.tr/index.php/alm/article/view/1075

Batur, M., & Alkan, R. M. (2024). Bibliometric analysis of the greatest nuclear disasters: What is known so far and what are the prospects? *The International Archives of the Photogrammetry, Remote Sensing and Spatial Information Sciences, 48*, 61–68. https://doi.org/10.5194/isprs-archives-XLVIII-4-W9-2024-61-2024

Batur, M., Alkan, R. M., Karaman, H., & Ozener, H. (2024). Recommendations for protective actions based on projected public health risks following a postulated nuclear power plant accident.

Malaysian Journal of Fundamental and Applied Sciences, 20(4), 923–938. https://doi.org/10.11113/mjfas.v20n4.3561

Batur, M., Alkan, R. M., Karaman, H., & Ozener, H. (2025). Multi-dimensional optimization of nuclear emergency shelters: Balancing capacity, evacuation efficiency, and supply accessibility. *International Journal of Engineering and Geosciences, 10*(2), 244–261. https://doi.org/10.26833/ijeg.1596244

Bektaş, S., & Lüle, S. Ş. (2022). An integrated method for atmospheric dispersion and corresponding risks: Application to ITU TRIGA Mark II research reactor. *Progress in Nuclear Energy, 143*, 104039. https://doi.org/10.1016/j.pnucene.2021.104039

Bucherie, A., Hultquist, C., Adamo, S., Neely, C., Ayala, F., Bazo, J., & Kruczkiewicz, A. (2022). A comparison of social vulnerability indices specific to flooding in Ecuador: Principal component analysis (PCA) and expert knowledge. *International Journal of Disaster Risk Reduction, 73*, 102897. https://doi.org/10.1016/j.ijdrr.2022.102897

Connors, L., & Zhang, C. H. (2023). A national analysis of the spatial patterns and correlates of evictions in the United States. *Applied Spatial Analysis and Policy, 16*(4), 1661–1682. https://doi.org/10.1007/s12061-023-09534-x

Contreras, D., Bhamidipati, S., & Wilkinson, S. (2023). Social vulnerability and spatial inequality in access to healthcare facilities: The case of the Santiago Metropolitan Region (RMS). *Chile. Socio-Economic Planning Sciences, 90*, 101735. https://doi.org/10.1016/j.seps.2023.101735

Das, D., Ojha, A. K., Kramsapi, H., Baruah, P. P., & Dutta, M. K. (2019). Road network analysis of Guwahati city using GIS. *SN Applied Sciences, 1*, 1–11. https://doi.org/10.1007/s42452-019-0907-4

Davies, M. (2001). Adaptive AHP: A review of marketing applications with extensions. *European Journal of Marketing, 35*(7/8), 872–894. https://doi.org/10.1108/EUM0000000005729

Debnath, B., Bari, A. M., de Jesus Pacheco, D. A., & Karmaker, C. L. (2023). An integrated Best-Worst Method and Interpretive Structural Modeling approach for assessing the barriers to circular economy implementation. *Decision Analytics Journal, 7*, 100250. https://doi.org/10.1016/j.dajour.2023.100250

FAO. (2011). *Guidelines for Food Safety and Quality in Emergency Situations*. Food and Agriculture Organization.

Fatemi, F., Ardalan, A., Aguirre, B., Mansouri, N., & Mohammadfam, I. (2017). Social vulnerability criterias in disasters: Findings from a systematic review. *International Journal of Disaster Risk Reduction, 22*, 219–227. https://doi.org/10.1016/j.ijdrr.2016.09.006

Fekete, A. (2019). Social vulnerability change assessment: Monitoring longitudinal demographic indicators of disaster risk in Germany from 2005 to 2015. *Natural Hazards, 95*(3), 585–614. https://doi.org/10.1007/s11069-018-3506-6

FEMA. (2019). *National Response Framework* (4th ed.). U.S. Department of Homeland Security.

Fraser, T., & Naquin, N. (2022). Better together? The role of social capital in urban social vulnerability. *Habitat International, 124*, 102561. https://doi.org/10.1016/j.habitatint.2022.102561

Frigerio, I., Zanini, F., Mattavelli, M., & De Amicis, M. (2019). Understanding the interacting factors that influence social vulnerability: A case study of the 2016 central Italy earthquake. *Disasters, 43*(4), 867–890. https://doi.org/10.1111/disa.12403

Fukasawa, M., Taniguchi, M. U., Akiyama, T., Horikoshi, N., Yasumura, S., Yabe, H., Kawakami, N. (2024). Social networks and posttraumatic stress symptoms five to ten years after the Fukushima nuclear power plant disaster. *Social Science & Medicine*, 117189. https://doi.org/10.1016/j.socscimed.2024.117189

Furlan, E., Dalla Pozza, P., Michetti, M., Torresan, S., Critto, A., & Marcomini, A. (2021). Development of a Multi-dimensional coastal vulnerability index: Assessing vulnerability to inundation scenarios in the Italian coast. *Science of the Total Environment, 772*, 144650. https://doi.org/10.1016/j.scitotenv.2020.144650

Gayen, S., Villalta, L. I. V., Haque, S. M. (2020). Comparative social vulnerability assessment in Purba Medinipur district, West Bengal, India. *European Journal of Geography*, *11*(1). https://doi.org/10.48088/ejg.s.gay.11.1.93.107

Guo, X., & Kapucu, N. (2020). Assessing social vulnerability to earthquake disaster using rough analytic hierarchy process method: A case study of Hanzhong City, China. *Safety Science, 125*, 104625. https://doi.org/10.1016/j.ssci.2020.104625

Hadipour, V., Vafaie, F., & Kerle, N. (2020). An criteria-based approach to assess social vulnerability of coastal areas to sea-level rise and flooding: A case study of Bandar Abbas city, Iran. *Ocean & Coastal Management, 188*, 105077. https://doi.org/10.1016/j.ocecoaman.2019.105077

Hasegawa, A., Ohira, T., Maeda, M., Yasumura, S., & Tanigawa, K. (2016). Emergency responses and health consequences after the Fukushima accident; evacuation and relocation. *Clinical Oncology, 28*(4), 237–244. https://doi.org/10.1016/j.clon.2016.01.002

He, B., & Guan, Q. (2024). Investigating the effects of spatial scales on social vulnerability index: A hybrid uncertainty and sensitivity analysis approach combined with remote sensing land cover data. *Risk Analysis, 44*(11), 2723–2739. https://doi.org/10.1111/risa.14342

IAEA. (2006). *Manual for first responders to a radiological emergency*. Vienna: International Atomic Energy Agency.

IAEA. (2015) Preparedness and response for a nuclear or radiological emergency. IAEA safety standards series No. GS-R-7. General Safety Requirements. International Atomic Energy Agency, Vienna

Isia, I., Hadibarata, T., Hapsari, R. I., Jusoh, M. N. H., Bhattacharjya, R. K., & Shahedan, N. F. (2023). Assessing social vulnerability to flood hazards: A case study of Sarawak's divisions. *International Journal of Disaster Risk Reduction, 97*, 104052. https://doi.org/10.1016/j.ijdrr.2023.104052

Jankowski, P. (1995). Integrating geographical information systems and multiple criteria decision-making methods. *International Journal of Geographical Information Systems, 9*(3), 251–273. https://doi.org/10.1080/02693799508902036

Jena, R., Pradhan, B., & Beydoun, G. (2020). Earthquake vulnerability assessment in Northern Sumatra province by using a multi-criteria decision-making model. *International Journal of Disaster Risk Reduction, 46*, 101518. https://doi.org/10.1016/j.ijdrr.2020.101518

Karaman, H., & Erden, T. (2014). Net earthquake hazard and elements at risk (NEaR) map creation for city of Istanbul via spatial multi-criteria decision analysis. *Natural Hazards, 73*, 685–709. https://doi.org/10.1007/s11069-014-1099-2

Kazibudzki, P. T. (2021). On the statistical discrepancy and affinity of priority vector heuristics in pairwise-comparison-based methods. *Entropy, 23*(9), 1150. https://doi.org/10.3390/e23091150

Kumar, D., & Bhattacharjya, R. K. (2020). Study of integrated social vulnerability index SoVI of hilly region of Uttarakhand, India. *Environmental and Climate Technologies, 24*(1), 105–122. https://doi.org/10.2478/rtuect-2020-0007

Li, D., Cova, T. J., & Dennison, P. E. (2019). Setting wildfire evacuation triggers by coupling fire and traffic simulation models: A spatiotemporal GIS approach. *Fire Technology, 55*, 617–642. https://doi.org/10.1007/s10694-018-0771-6

Malczewski, J. (1999). *GIS and Multicriteria Decision Analysis*. John Wiley & Sons Inc.

Müller, A., Reiter, J., & Weiland, U. (2011). Assessment of urban vulnerability towards floods using an criteria-based approach–a case study for Santiago de Chile. *Natural Hazards and Earth System Sciences, 11*(8), 2107–2123. https://doi.org/10.5194/nhess-11-2107-2011

Nazeer, M., & Bork, H. R. (2019). Flood vulnerability assessment through different methodological approaches in the context of North-West Khyber Pakhtunkhwa, Pakistan. *Sustainability, 11*(23), 6695. https://doi.org/10.3390/su11236695

Nguyen, C. V., Horne, R., Fien, J., & Cheong, F. (2017). Assessment of social vulnerability to climate change at the local scale: Development and application of a Social Vulnerability Index. *Climatic Change, 143*, 355–370. https://doi.org/10.1007/s10584-017-2012-2

Ohba, T., Tanigawa, K., & Liutsko, L. (2021). Evacuation after a nuclear accident: Critical reviews of past nuclear accidents and proposal for future planning. *Environment International, 148*, 106379. https://doi.org/10.1016/j.envint.2021.106379

Oktari, R. S., Munadi, K., Idroes, R., & Sofyan, H. (2020). Knowledge management practices in disaster management: Systematic review. *International Journal of Disaster Risk Reduction, 51*, 101881. https://doi.org/10.1016/j.ijdrr.2020.101881

Oloruntoba, R., Sridharan, R., & Davison, G. (2018). A proposed framework of key activities and processes in the preparedness and recovery phases of disaster management. *Disasters, 42*(3), 541–570. https://doi.org/10.1111/disa.12268

Orhan, O. (2021). Land suitability determination for citrus cultivation using a GIS-based multi-criteria analysis in Mersin, Turkey. *Computers and Electronics in Agriculture, 190*, 106433. https://doi.org/10.1016/j.compag.2021.106433

Ortega, J., Moslem, S., Palaguachi, J., Ortega, M., Campisi, T., & Torrisi, V. (2021). An integrated multi criteria decision making model for evaluating park-and-ride facility location issue: A case study for cuenca city in Ecuador. *Sustainability, 13*(13), 7461. https://doi.org/10.3390/su13137461

Park, S., Sohn, S., & Jae, M. (2021). Cohort-based evacuation time estimation using TSIS-CORSIM. *Nuclear Engineering and Technology, 53*(6), 1979–1990. https://doi.org/10.1016/j.net.2020.11.028

Rezaei, J. (2015). Best-worst multi-criteria decision-making method. *Omega, 53*, 49–57. https://doi.org/10.1016/j.omega.2014.11.009

Rufat, S., Tate, E., Emrich, C. T., & Antolini, F. (2019). How valid are social vulnerability models? *Annals of the American Association of Geographers, 109*(4), 1131–1153. https://doi.org/10.1080/24694452.2018.1535887

Saaty, T. L. (1977). A scaling method for priorities in hierarchical structures. *Journal of Mathematical Psychology, 15*(3), 234–281. https://doi.org/10.1016/0022-2496(77)90033-5

Sauti, N. S., Daud, M. E., & Kaamin, M. (2020). Construction of an integrated social vulnerability index to identify spatial variability of exposure to seismic hazard in Pahang, Malaysia. *International Journal of Design & Nature and Ecodynamics, 15*(3), 365–372. https://doi.org/10.18280/ijdne.150310

Shafapourtehrany, M., Yariyan, P., Ozener, H., Pradhan, B., & Shabani, F. (2022). Evaluating the application of K-mean clustering in Earthquake vulnerability mapping of Istanbul, Turkey. *International Journal of Disaster Risk Reduction, 79*, 103154. https://doi.org/10.1016/j.ijdrr.2022.103154

Singh, M., & Pant, M. (2021). A review of selected weighing methods in MCDM with a case study. *International Journal of System Assurance Engineering and Management, 12*, 126–144. https://doi.org/10.1007/s13198-020-01033-3

Smith, J. N., Brown, R. M., Williams, W. J., Robert, M., Nelson, R., & Moran, S. B. (2015). Arrival of the Fukushima radioactivity plume in North American continental waters. *Proceedings of the National Academy of Sciences, 112*(5), 1310–1315. https://doi.org/10.1073/pnas.1412814112

Starczewski, T. (2023). Simulation research on the relationship between selected inconsistency indices used in AHP. *Entropy, 25*(10), 1464. https://doi.org/10.3390/e25101464

Steer, K., Abebe, E., Almashor, M., Beloglazov, A., & Zhong, X. (2017). On the utility of shelters in wildfire evacuations. *Fire Safety Journal, 94*, 22–32. https://doi.org/10.1016/j.firesaf.2017.09.001

Taheri, S. M., & Hesamian, G. (2013). A generalization of the Wilcoxon signed-rank test and its applications. *Statistical Papers, 54*, 457–470. https://doi.org/10.1007/s00362-012-0443-4

Tascón-González, L., Ferrer-Julià, M., Ruiz, M., & García-Meléndez, E. (2020). Social vulnerability assessment for flood risk analysis. *Water, 12*(2), 558. https://doi.org/10.3390/w12020558

Tate, E. (2012). Social vulnerability indices: A comparative assessment using uncertainty and sensitivity analysis. *Natural Hazards, 63*, 325–347. https://doi.org/10.1007/s11069-012-0152-2

Tuncer, B., Akkaya, A. D., Yucemen, M. S. (2024). Multicriteria decision making in site selection for nuclear power plants. *Nuclear Technology*, 1–26. https://doi.org/10.1080/00295450.2023.2299078

Turkish Statistical Institute (2023). Transportation statistics. Accessed January, 2023.

UNDRR. (2015). *Sendai Framework for Disaster Risk Reduction 2015–2030*. United Nations Office for Disaster Risk Reduction.

WHO. (2017). *Health Emergency and Disaster Risk Management Framework*. World Health Organization.

Wilson, R. T., LaBarge, B. L., Stahl, L. E., Goldenberg, D., Lyamzina, Y., & Talbott, E. O. (2023). What have we learned about health effects more than 40 years after the Three Mile Island nuclear accident? A scoping and process review. *Risk, Hazards & Crisis in Public Policy, 14*(2), 129–158. https://doi.org/10.1002/rhc3.12258

Xie, W., & Meng, Q. (2023). An integrated PCA-AHP method to assess urban social vulnerability to sea level rise risks in Tampa, Florida. *Sustainability, 15*(3), 2400. https://doi.org/10.3390/su15032400

Zehra, S. N., & Wong, S. D. (2024). Systematic review and research gaps on wildfire evacuations: Infrastructure, transportation modes, networks, and planning. *Transportation Planning and Technology, 47*(8), 1–35. https://doi.org/10.1080/03081060.2024.2348713

Žurovec, O., Čadro, S., & Sitaula, B. K. (2017). Quantitative assessment of vulnerability to climate change in rural municipalities of Bosnia and Herzegovina. *Sustainability, 9*(7), 1208. https://doi.org/10.3390/su9071208

Publisher's Note Springer Nature remains neutral with regard to jurisdictional claims in published maps and institutional affiliations.